0098

Environment Canada
Water Science and Technology Directorate

Direction générale des sciences et de la technologie, eau
Environnement Canada

Coastal Boundary Layer Characteristics During Summer Stratification in Lake Ontario

By:
Y.R. Rao & C.R. Murthy

NWRI Contribution # 00-98

TD
226
N87
no.
00-98

0-98

Coastal Boundary Layer Characteristics During Summer Stratification in Lake Ontario

Y.R. Rao and C.R. Murthy
National Water Research Institute
867 Lakeshore Road
Burlington, Ontario
Canada, L7R 4A6

NWRI Cont. # 00-98

Coastal Boundary Layer Characteristics During Summer Stratification in Lake Ontario

Y.R. Rao and C.R. Murthy

MANAGEMENT PERSPECTIVE

The north shore of Lake Ontario is heavily urbanised and industrialised including Pickering and Darlington Nuclear Generating Stations and thus large quantities of nearshore waters are drawn. The municipal and industrial waste water effluents are then discharged into the lake. Characterising the base line climatology of nearshore currents, dispersal properties is essential to assess the deleterious effects of the pollutants on the north shore coastal ecosystem. The north shore of Lake Ontario exhibits a typical coastal boundary layer, where the nearshore currents are shore parallel and reach a peak around 2-3km from the shore. Simultaneous measurements of currents using fixed point current meters and drifting buoys are applied to delineate the structure of the coastal boundary layer and parameterise the nearshore currents and dispersal capacity appropriate for developing coastal outfall models for MWWE and industrial effluents. The results are derived from sound physical limnological principles and thus can be applied in similar near shore areas.

Abstract

Simultaneous measurements of Eulerian and Lagrangian currents along the north shore of Lake Ontario are analyzed to provide the mean flow properties and horizontal turbulent exchange characteristics in the coastal boundary layer (CBL). The summer coastal boundary layer is characterized by a frictional boundary layer (FBL) of a width of ~3km, in which shore and bottom friction affects the flow. In this regime the currents are predominantly shore parallel and persistent. The outer boundary layer also called as an inertial boundary layer (IBL) which is typically of the order of 5-6 km wide, is a consequence of the adjustment of inertial oscillations to the lateral boundary.

During the summer season within the CBL, the current motions are associated with thermocline displacements. The eastward (westward) wind stress causes thermocline elevation (depression) causing upwelling (downwelling). The mean sub-surface westward currents associated with downwelling events are typically stronger in comparison to weak eastward flow during upwelling. Further, upwelling events are characterized by reduced low frequency motion (> 1day) and significant near-inertial (~17 hr) currents. The width of the CBL decreases during upwelling and increases during downwelling. Internal waves generated by baroclinic seiches during these events have periods from 11 to 17 hours. The near-surface horizontal exchange coefficients calculated from Lagrangian measurements are higher than those from sub-surface Eulerian values. Upwelling events show that the turbulent kinetic energy is higher than mean flow kinetic energy (MKE) in the CBL, and cross-shore turbulent exchange increases in the IBL. During downwelling the alongshore exchange coefficients are higher in the FBL, whereas cross-shore exchanges are higher in the IBL. Downwelling events are also characterized by increased contribution from the MKE than the TKE.

Caractéristiques de la couche limite riveraine pendant la stratification d'été dans le lac Ontario

Y.R. Rao et C.R. Murthy

SOMMAIRE À L'INTENTION DE LA DIRECTION

La rive nord du lac Ontario est une zone fortement urbanisée et industrialisée englobant les centrales nucléaires de Pickering et de Darlington, qui soutirent de grandes quantités d'eau à proximité des rives, et les effluents d'eaux usées municipales et industrielles sont ensuite déversés dans le lac. La détermination des caractéristiques climatologiques de base des courants riverains et des propriétés de dispersion est essentielle pour évaluer les effets nuisibles des polluants dans les écosystèmes de la rive nord du lac Ontario. Sur celle-ci, on trouve une couche limite riveraine typique, où les courants riverains sont parallèles au rivage et atteignent un maximum à environ 2 – 3 km au large. On effectue des mesures simultanées des courants à l'aide de courantomètres fixes et de bouées dérivantes afin de délimiter la structure de la couche limite riveraine et de paramétriser les courants riverains et la capacité de dispersion, afin de faciliter le développement de modèles d'exutoires riverains pour les effluents des SEEU et des industries. On peut donc appliquer ces résultats à des zones riveraines semblables, parce qu'ils sont fondés sur des principes de limnologie physique éprouvés.

RÉSUMÉ

On analyse des mesures simultanées de courants eulériens et lagrangiens le long de la rive nord du lac Ontario afin de déterminer les propriétés de l'écoulement moyen et les caractéristiques d'échange turbulent horizontal dans la couche limite riveraine (CLR). La couche limite riveraine d'été est caractérisée par une couche limite de frottement (CLF) d'une largeur d'environ 3 km, dans laquelle le frottement du rivage et du fond ralentit l'écoulement. Ce régime favorise surtout les courants parallèles au rivage et persistants. La couche limite extérieure, également appelée " couche limite inertielle " (CLI), dont la largeur type est de l'ordre de 5 à 6 km, est créée par l'ajustement des oscillations inertielles à la limite latérale.
Pendant l'été, à l'intérieur de la CLR, les mouvements des courants sont associés aux déplacements de la thermocline. La tension du vent vers l'est (ou vers l'ouest) entraîne une élévation (ou une dépression) de la thermocline qui cause des remontées (ou des plongées) d'eau. Les courants moyens de subsurface dirigés vers l'ouest associés aux épisodes de plongée d'eau sont normalement plus forts que les écoulements faibles dirigés vers l'est pendant les épisodes de remontée d'eau. En outre, ces derniers sont caractérisés par des déplacements réduits à basse fréquence (moins d'un jour) et par des courants quasi-inertiels significatifs (d'environ 17 h). La largeur de la CLR diminue pendant les remontées et augmente pendant les plongées. Au cours de ces épisodes, on observait des ondes internes, à périodes de 11 à 17 heures, générées par des seiches baroclíniques. Les coefficients d'échange horizontal près de la surface, calculés à partir des mesures lagrangiennes, sont plus élevés que ceux calculés à partir des mesures eulériennes de la subsurface. Les épisodes de remontée d'eau indiquent que l'énergie cynétique turbulente est plus forte que l'énergie cynétique moyenne de l'écoulement (ECME) dans la CLR, et que les échanges turbulents perpendiculaires au rivage augmentent dans la CLI. Pendant les épisodes de plongée d'eau, les coefficients d'échange le long du rivage sont plus élevés dans la CLF, alors que ceux des échanges perpendiculaires au rivage sont plus élevés dans la CLI. De plus, les épisodes de plongée d'eau sont caractérisés par une contribution accrue de l'ECM, par rapport à l'énergie cynétique totale de l'écoulement (ECTE).

1.0 **Introduction**

Coastal zones are areas of intense biological, chemical and geological processing of materials arriving from both the terrestrial and offshore zones. Details of the transport and pathways of material entering to the coastal environment are dictated by complex coastal currents and forcing functions in a distinct inshore region known as the coastal boundary layer (Csanady, 1972) or the inner shelf (Lentz, 1995). The significant features of the coastal zone are across-shelf exchange and strong shore parallel currents. The large enclosed and rotating basins like the Great Lakes are subjected to many of the same forcings as coastal oceans and serve as an example for understanding the complicated coastal ocean dynamics. They are also easier to study than coastal ocean because they are smaller and do not have salinity effects and tides (Csanady, 1982; Beletsky et al., 1997). The Great Lakes manifest into two distinct flow environments: an open lake environment and a coastal environment. The main differences between these regions is that the momentum imparted by the wind stress is balanced by bottom friction inshore, while it is balanced by the Coriolis force offshore.

The thermal structure and circulation in the Great Lakes generally depends on the season because of the large annual variation of surface fluxes (Boyce et al., 1989). During the unstratified period (November-June), storm action is the most important forcing, as higher wind speeds and the absence of stratification allow the wind forcing to penetrate deeper into the water column. In summer and fall there is a distinct thermocline in the upper 30 m in most of the lakes which makes them stratified. During this period of stratification, significant wind events will cause upwelling and downwelling of the thermocline along the shore. The scale of the offshore distance over which these events takes place depends on the wind stress and near shore bathymetry, and is typically of the order of 5-10 km, hence, within the coastal boundary layer (Murthy and Dunbar, 1981). In the coastal upwelling zone a near balance exists between wind stress, Coriolis force and internal pressure gradient. However, as the wind subsides two types of waves are established: the Poincare' wave and the internal Kelvin wave. Poincare' waves are basin wide response with oscillations in the thermocline across the entire lake with anti-cyclonic phase propagation. On the other hand, internal Kelvin waves are coastally trapped response of the thermocline that progresses cyclonically around the lake. The Rossby radius of deformation which is typically of the order of 3-5 km in the Great Lakes is the e-folding scale for the amplitude of this wave as a function of distance from shore.

Past studies on the mean summer circulation in the coastal zone of Lake Ontario were based on daily transect data collected during the International Field Year on Great Lakes (IFYGL) in 1972. Although some important features of mean flow pattern were explained using this data and simple equilibrium models, many discrepancies were observed between model results and measurements owing to transient upwelling and downwelling events during summer (Csanady and Scott, 1980). Further, upwelling and downwelling events have also been cited as some of the important mechanisms for onshore and offshore transport of sediment (Lee and Hawley, 1998). Observational and theoretical studies of coastal upwelling and downwelling for deciphering physical dynamics near a coast were carried out in several coastal regions (Smith, 1981; Brink et al., 1980; Winant et al., 1987; Allen et al., 1995; Allen and Newberger, 1996). In the Great Lakes the coastal upwelling and downwelling induced by local winds and propagation of these events as internal Kelvin waves have also been studied by using both field data and numerical models (Blanton, 1975;

Csanady, 1982; Simons and Schertzer, 1989; Beletsky et al., 1997). However, the elucidation of the role of physical processes during these episodes in the distribution of geologically and biologically important materials in the coastal zones of the Great Lakes has not been attempted in great detail mainly due to lack of detailed time series measurements.

The purpose of this paper is to provide a description of the structure of flow within the coastal boundary layer during the summer regime in Lake Ontario using simultaneous Eulerian and Lagrangian currents. These data records are analyzed to identify the characteristics of mean and fluctuating currents and temperature during upwelling and downwelling cycles. This study uses near-surface drifter observations along with moored current meter statistics in the coastal zone of Lake Ontario. A quantitative analysis of dynamical balances and exchange characteristics for upwelling and downwelling events would enhance the understanding of horizontal exchange processes in the coastal zone. The remainder of this paper is divided into five sections. The next section gives a brief description of data and methods followed by mean circulation and exchange characteristics of the summer regime obtained from Eulerian measurements. The detailed flow and structure of the coastal boundary layer during upwelling and downwelling events are discussed in section 4, followed by a section on the calculation of Lagrangian and Eulerian exchange coefficients during these episodes. The last section gives a brief summary and conclusions of this study.

2.0 Data and Methods

The data consists of Eulerian time series of water temperature and currents (speed and direction) obtained from an array of 6 SACM Brown current meters moored at a depth of 10 m off Darlington Nuclear Generating Station on the north shore of Lake Ontario (figure 1). At this coastal site the bathymetry gently slopes from a depth of 11m at the innermost mooring to 87.5m at the outermost. The coastal chain was deployed perpendicular to the local bathymetry and extended to 14.3 km offshore. The sampling rate of the current data was 30 minutes, except at the second mooring from the shore where the rate was 36 minutes. We have obtained current and temperature data from 1 July 1990 (Julian Day 181) to 30 September 1990 (Julian Day 273) for this analysis. The coordinate system used is such that the x-axis is parallel to the shore and y-axis is pointed offshore along the instrument array. The time series is first hourly averaged, then the east and north velocities are resolved into shore parallel and shore perpendicular components after aligning to the local shore line (80° from north). Figure 1 also shows flow ellipses in the alongshore and cross-shore directions for all current meters. This gives an estimate of predominant movements of water along the northshore of Lake Ontario. The experiment also contained temperature survey component along the coastal chain stations.

A land based tower at Toronto Island airport provided hourly wind speeds and directions from 1 July 1990 to 30 September 1990. Since the scale of the atmospheric weather systems are typically larger than Lake Ontario, the wind field may be expected to be rather uniform over the lake (Simons and Schertzer, 1989). Thus the winds at this island station should be representative of forcing during this period. The vector wind stress was estimated as $\tau = \rho_a C_d |W| W$, where ρ_a is the air density, C_d is a constant drag coefficient of $1.3*10^{-3}$ and W is the wind velocity. Here the direction of the wind stress points toward the reference. The stresses were also decomposed into alongshore and cross-shore components with alongshore direction being aligned with the general orientation of the north shore (80° from north) of Lake Ontario.

The current data were supplemented by six Lagrangian drifter experiments conducted along a line on the north shore of Lake Ontario during the period of May 1990 to October 1990. Seven to eight drifters were used in each experiment with drogues set at 3.5 m depth and were tracked using service Argos navigation. The drag area ratio for the Hermes Electronics drifters was estimated to be approximately 20:1 indicating the velocity errors arising out of wind drag is minimal (Niiler et al., 1995). There were on average 10 to 12 positional fixes per day per buoy. Out of the six experiments, two were chosen to study upwelling and downwelling characteristics. Each experiment lasted for a period of 8 to 10 days. In order to resolve the currents into shore parallel and perpendicular directions, the position time series was first converted to a velocity time series, in the form (S,θ), where S is the speed in cm/s and θ is the instantaneous direction in degrees measured from north. The velocity field was then resolved into alongshore and cross-shore components.

3.0 **Summer Regime**

In order to delineate parameters characteristic of transport and exchange processes, it is necessary to isolate the mean flow from the time series data. Numerical filtering techniques developed by Graham (1963) and extensively applied to the analysis of large lakes by Simons (1974) were used to define mean flow and fluctuations. The filter was designed on the basis of typical kinetic energy spectra constructed from 92 days of hourly current meter data from the six coastal chain current meter stations.

Typical plots of kinetic energy spectra of along-shore and cross-shore components along the coastal chain moorings are plotted in figure 2a and 2b, respectively. The energy spectra were characterized by a flat peak around 10-12 days (0.0041-0.0034 cph) and a spectral minimum around 24-30 hours (0.04 - 0.03 cph). The dominant peak near 17 hr

(0.058 cph) corresponds to the near-inertial period of Lake Ontario and increases offshore. The spectral minimum at 24 to 30 hours is a characteristic feature of energy transfer from large scale lake wide circulation to small scale oscillations. The period corresponding to the spectral minimum can be used as a transition between mean flow and fluctuations. The low-pass filter with a cutoff frequency of 0.055 - 0.041 cph (18 to 24 hr) leaves all high frequency oscillations including inertial oscillations in the fluctuating part. Although near-inertial oscillations are more like an organized flow, because of their oscillatory nature they can be viewed as large-scale fluctuations and as such contribute to dispersal processes, hence, they are included in fluctuating turbulent currents (Murthy and Dunbar, 1981). The time series of mean (filtered) currents shows that along-shore currents were dominant at all six stations, and cross-shore velocities account for less than 10% of all subsurface current intensities in the first 10 km from shore (Fig 3). The nearshore stations (within 3.5 km from shore) show that alongshore currents were dominated by low frequency motion (> 3 days) more than offshore stations. The kinetic energy of the alongshore flow in the low frequency band accounts for more than 95% of the total kinetic energy, indicating the shore-parallel nature of currents.

We have next examined the response of currents to wind forcing. The coherence between alongshore and cross-shore winds with alongshore currents was calculated for all stations. Examples of coherence plots at stations 2 and 6 are shown in figures 2c & d. Significant response to alongshore wind forcing occurs in the low frequency band (high coherence) at all stations. Cross-shore winds were mainly coherent with alongshore currents in the low frequency band. In the high frequency band significant coherence was noticed at near-inertial frequencies in both alongshore and cross-shore cases showing the influence of winds on the rotary near-inertial motion. Further, horizontal coherence between all current meters with reference to station 2 (not shown), shows that alongshore currents were highly coherent (coherence > 0.90) and in phase for stations located from 3 km to 10 km offshore in low frequency (> 3 day) and near-inertial domains. However, the currents at the inner coastal station were not significantly coherent with those at other locations along the coastal chain.

Figure 4a shows the variations of mean cross-shore and alongshore current components with distance from shore. The cross-shore velocity increased with offshore and peaked at 5 km from shore. The mean alongshore currents were toward the west and peaked at a distance of 3 km from shore. The observed westward mean flow of 3 to 4 cm/s was consistent with earlier observations of mean cyclonic circulation in large lakes, attributed by Emery and Csanady (1973) to mean cyclonic curl in the wind stress field. On the other hand, Wunsch (1970) proposed that the Lagrangian drift associated with internal Kelvin waves might account for net cyclonic drift. Csanady (1982) attributed this flow to the persistence of domed thermocline in summer due to the influence of prevailing winds. Presence of this domed thermocline in coastal waters is evidence of adjustment to geostrophic equilibrium provided by cyclonic circulation with mean surface flow of 3-4 cm/s. Recent experiments using three dimensional numerical models have shown that the certain selections of surface and bottom boundary conditions and vertical mixing yield mean cyclonic circulation in large lakes (Schwab et al., 1995; Davidson et al., 1998).

Figure 4b shows components of kinetic energy (total, mean and fluctuations) as a function of offshore distance. The mean flow kinetic energy (MKE) dominates within 8-10 km from the shore. Fluctuating kinetic energy or turbulent kinetic energy (TKE) increases with offshore distance, as near-inertial oscillations become dominant offshore. In summer the MKE increases offshore to a peak at about 3 km from shore then decreases further offshore. Murthy and Dunbar (1981) characterized this flow regime, where total kinetic energy or mean currents increases to a peak as the frictional boundary layer (FBL). Within this zone the currents are influenced by bottom and shore friction. Beyond 3 km, due to the adjustment of inertial oscillations to shore parallel flow an outer boundary layer develops, known as the inertial boundary layer (IBL). The total (FBL+IBL) forms the coastal boundary layer (CBL). In defining the width of the IBL previous studies used the distance where the inertial oscillations dominate the shore parallel flow. Alternatively, the CBL width can be simply taken as the distance where TKE contributes maximum to the total kinetic energy. During the summer stratification in Lake Ontario the width of the CBL as determined here was around 10 km, which is consistent with earlier observations (Csanady, 1972).

In order to quantify the turbulence levels in the flow, we define the relative intensity or turbulent coefficients given as $i_u = \sqrt{\overline{u'^2}} / \bar{s}$ and $i_v = \sqrt{\overline{v'^2}} / \bar{s}$. Here, u′ and v′ are the fluctuating part of along-shore and cross-shore currents and $\bar{s}$ is the scalar mean speed. The turbulence intensity coefficients are relatively larger as we go offshore due to increased contributions from near-inertial oscillations (fig. 4c). Although the near shore station at a depth of 11m has shown slightly higher intensities due to shore and bottom frictional influences, they were not remarkably high as observed in Lake Huron (Murthy and Dunbar, 1981). The magnitudes of alongshore and cross-shore turbulent intensities increase with offshore and near-isotropic within the CBL. This is in contrast to drifter observations made on the northern California shelf which showed approximate isotropy at 40 km from shore and non-isotropy in the inner shelf (Davis, 1985).

4.0 Analysis of Upwelling and Downwelling events

The position of the 10°C or 13°C isotherm (thermocline) has generally been used to define upwelling and downwelling episodes in Lake Ontario (Blanton, 1975; Simons and Schertzer, 1989). During this observational programme water temperature was measured along with subsurface currents at 10 m depth in the coastal chain stations, with occasional ship based temperature profile measurement surveys. As an example the cross-sectional thermal structure obtained from several temperature transects during an upwelling event from 23 to 24 July 1990 and downwelling on 17 Aug 1990 are shown in figures 5a & 5b, respectively. During upwelling the thermocline was displaced to surface layers with the 13°C isotherm intersecting the surface in the near shore region. The strong eastward wind stress of 1-2 dynes/cm^2 for nearly two days raised the thermocline and displaced warmer waters offshore . During the downwelling event the thermocline shifted to 16-20 m depth with downward tilt near the shore.

Figures 5c &d show the hourly variations of wind stress and lowpass filtered temperature data at selected stations. The alongshore winds were primarily responsible for upwelling and downwelling of isotherms. The near coastal stations responded more to these events than offshore stations. The eastward (westward) wind stress causes thermocline elevation (depression) indicating upwelling (downwelling) of isotherms. The upwelling events were characterized by eastward flowing sub-surface currents and downwelling events by strong westward flowing currents (Fig. 3). These upwelling/downwelling events were common during the summer regime, with each episode lasting 4-6 days on average. Although certain upwelling and downwelling events were influenced by favorable local winds, during relatively calm (weak) wind epochs, we observe warmer currents flowing westward. In the spectral analysis of currents (fig 2a) a 10-12 day periodicity was observed, which may be due to the presence of internal Kelvin wave (Csanady, 1982). The westward current reversals in the CBL took on average 24-30 hours suggesting that the wave length of Kelvin wave system could be of the order of 50-100 km. This was also reflected in the thermocline excursions of 10-15 m from upwelling to downwelling in 4-5 days. Surface temperatures obtained from satellite pictures during these events also show this phenomenon with upwelling (~10°C) along the north shore and downwelling (19-20°C) along the south shore or *vice-versa* with similar scales. Two such upwelling and downwelling episodes along the north shore, during which both Eulerian and Lagrangian measurements were available, have been selected for detailed analysis of flow and turbulent exchange characteristics.

4.1 *Upwelling episode*

Eight drifters were deployed close to the current meter moorings in the Darlington coastal chain on 17 July 1990 and were recovered on 26 July 1990. The eastward wind stress from July 15 caused an upwelling of the thermocline by rapidly dropping the temperature by 6-8°C in the near coastal stations. The mean sub-surface currents over this period changed to eastward except at the innermost station. The hourly time series of drifter positions are plotted in figure 6. The drifters traveled south-eastward with nearshore trajectories showing shore parallel currents, while offshore drifters oscillated at the inertial period. The surface flow obtained from drifters shows offshore directed flow (-4.4 cm/s) during peak upwelling indicating that surface winds displaced the warmer waters offshore and caused the interface to move upward within the Rossby radius of deformation. Weak onshore flow was observed at stations 3 and 5 at 10 m depth. The south-eastward flow in surface layers and weak return flow at 10 m depth at a few stations suggest that the coastal divergence at the surface during upwelling period is compensated at sub-surface levels. This is consistent with the observations in the surface mixed layer of different coastal regions (Lentz, 1992 and Allen et al., 1995). The mean Eulerian currents in near coastal stations during this episode were rather weak. As such no coastal jet emerges from this analysis, although slightly higher velocities were observed 3-4 km from shore. The absence of strong coastal jet during this episode can be due to the shallow nature of the thermocline and also possibly to internal friction (Csanady, 1982).

In order to compare the Lagrangian currents at 3.5 m and Eulerian currents at 10m depth, we have low-pass filtered the drifter currents and calculated mean currents for each drifter when they are in 20.0 km in alongshore and 2.0 km in cross-shore bins centered on the respective current meters (Dever et al., 1998). Table 1 presents the statistics of mean and fluctuating currents from both experiments during upwelling. The mean along-shore and cross-shore current components obtained in the surface level (3.5 m) from drifters were higher than Eulerian values at 10 m depth indicating the existence of shear in the upper mixed layer. The fluctuating velocities were higher than mean currents in both Lagrangian and Eulerian measurements. This may be because of the Lagrangian measurements were conducted in surface levels at 3.5 m depth, and hence were more influenced by prevailing winds. Other explanations may be equally plausible (Davis, 1985, 1991). Few current meters were located in the thermocline region due to its upward movement during upwelling. Differences between drifter and current meter velocities also arise owing to wave effects. Drifters at this depth are generally affected by Stokes drift, however, estimates of wave-induced velocity differences due to Stokes drift were not attempted in this paper. Pal *et al* (manuscript submitted to *J. Geophys. Res.*, 1999) observed that the differences between drifter currents and current meter values during this period were mainly due to depth differences and, to a limited extent to spatial variation and instrument errors. The rms values which are mainly due to near-inertial oscillations are higher at 3.5 m depth than at 10 m depth suggesting a downward propagation of internal wave energy during this episode.

Figure 7a shows the plots of sub-surface total kinetic energy, turbulent kinetic energy, and mean flow kinetic energy with distance offshore during the upwelling episode. Although total kinetic energy levels were comparatively less than summer values, the peak has shifted to 5.5 km from shore. The peak of the MKE also shifted to this distance indicating the width of the FBL. Unlike observed in mean summer conditions, episodes turbulent kinetic energy during the upwelling increased in the first 5.5 km, and then reduced significantly in the next 2-3 km, and again increased further offshore. The width of the CBL during this episode reduced to 9 km. Turbulent kinetic energy was comparable to mean kinetic energy in the first 3 km from shore, and in the rest of the CBL, turbulent kinetic energy contributed more than 65% to the total kinetic energy.

Figure 7b shows significant increase in turbulence intensity and near-isotropic conditions of turbulence within the CBL. Outside the coastal boundary layer the turbulent intensities sharply dropped to small values. The high values of turbulent intensity in the CBL, which was also reflected in high TKE values, was primarily due to increased near-inertial oscillations and reduced mean scalar current speed during this cycle. The peak of turbulent intensity slightly shifted to inshore compared to the summer regime. It may be noted that during an upwelling cycle the cross-shore turbulent intensity was slightly higher at the near coastal station and again outside the frictional boundary layer.

Near-inertial oscillations

Upwelling and downwelling of the thermocline represents a deviation from equilibrium due to the influence of wind stress. Once the winds subside, internal waves of clockwise motion will develop and contribute to the decay of kinetic energy. Ivey (1987) observed that mixing at ocean boundaries may be due to the reflection of internal waves or to the interaction of mean flow with the bottom. Recently, Bogucki et al (1997) also observed sediment resuspension by breaking internal solitary waves during upwelling on the California shelf. Further, Lee and Hawley (1998) noted that mean upwelling currents by themselves did not resuspended bottom material in Lake Michigan and speculated that near-inertial internal waves could be a possible mechanism for resuspension. Although short period oscillations in the near-inertial band (11-18 hrs) were analyzed by a few earlier studies in large lakes (Mortimer, 1977) their structure was not fully explored during these events (Blanton, 1975). Since it was observed that standard spectral analysis fails to detect different frequencies in the inertial band, earlier studies used a best fit method for Poincare′ modes. We used both power spectrum analysis with high resolution and a frequency search method. In the frequency search method a fast orthogonal search algorithm (Adeney and Korenberg, 1994) was used to a set of candidate frequencies ranging from 11 hr to 17.5 hr for two different upwelling and downwelling episodes. In this method a modified Gram-Schmidt procedure is used to create an orthogonal basis for arranging the time series. The most significant frequencies were obtained by reducing the mean square error between observations and model fit. The periods for candidate frequencies for some internal waves were based on the theoretical values for Lake Ontario (Schwab, 1977). For this study the inertial period was taken as 17.4 hr and the transverse baroclinic seiches (Poincare' type oscillations) with 1 to 5 modes were taken to be 16.9, 15.7, 14.2, 12.7 and 11.2 hr periods.

During the upwelling the kinetic energy of the fluctuations slightly increased due to the increase in near-inertial oscillations. Federuik and Allen (1996) observed similar increase in their model study over the Oregon continental shelf. Upwelling events were mainly characterized by a 16-hr (4-5 cm/s) wave in the CBL. Less significant, 16.9 hr (~ 2.5 cm/s) and 14.2 hr (~2 cm/s) waves were also observed at many stations. The amplitudes and phases of these waves varied all along the coastal chain stations. The station outside the CBL was mainly influenced by inertial waves with 17.3 hr periodicity, whereas the near coastal station was dominated by relatively shorter period waves (11 hr). The 14.2 hr wave was observed at the station 3.4 km from shore in most of the upwelling events. Temperature data also showed main oscillations at 16-hr and 17-hr periodicity. During the initial phase of upwelling events, the short bursts of eastward winds generated waves of period 11.2 hr and 14.2 hr, which were later replaced by more regular16.0-hr and 17-hr waves. This probably suggests that the short wind bursts generate higher mode baroclinic waves in the initial phase, which will be replaced by more regular waves. These observations also show the absence of pure inertial motion within the CBL.

4.2 *Downwelling episode*

During the downwelling episode eight drifters were deployed on August 16, 1990 and recovered on August 23, 1990 near the same stations as in upwelling case. The initial eastward winds from August 14 to 15 caused a strong upwelling of isotherms along the north shore of Lake Ontario. The cool temperatures prevailed for two more days even though the winds subsided. This was followed by strong westward winds from Aug 17 which caused an increase in water temperatures of 10-12°C in two days. This downwelling event was associated with strong westward currents of the order of 30-40 cm/s at some stations (see Fig 3). The hourly time series of drifter positions are shown in figure 8. The near shore drifters traveled westward under the influence of predominantly shore parallel currents, and the offshore drifters oscillated at near-inertial frequency.

Figure 9a shows the components of kinetic energy obtained from Eulerian measurements as a function of offshore distance. During downwelling mean kinetic energy sharply increased to a peak at 3 km from shore, thus dividing FBL and IBL regimes. The width of the CBL extended over 14 km during this episode. The turbulent kinetic energy was smaller than summer regime in the FBL, but comparable in the IBL. The contribution from the turbulent kinetic energy was less than 5% within the FBL during these events. Outside the CBL turbulent kinetic energy and mean kinetic energy were more or less of equal magnitude. Figure 9b shows decreased turbulent intensities all through the CBL. This is mainly due to decreased fluctuating velocities and increased mean currents.

Table 2 shows that the mean Eulerian alongshore currents were towards west with a coastal jet concentrated near 3 km from the shore. This episode shows that the CBL characteristics are similar to the summer regime with increased current speeds. It may be observed from Lagrangian and Eulerian currents that the mean currents at 10 m depth were much stronger than surface currents supporting the fact that downwelling currents extend over the deeper levels (Allen and Newberger, 1996). The mean surface currents flowed onshore, whereas the currents at 10 m depth outside the FBL showed offshore flow. Eulerian currents show non-isotropic nature of turbulence, with the along-shore component dominating over the cross-shore component in the CBL. Eulerian currents also showed that rms values of fluctuating velocities, although comparable to summer regime were much less than mean currents, thereby decreasing the turbulence intensities within the CBL.

Near-inertial oscillations

The short period near-inertial oscillations were studied during downwelling events as done in upwelling episodes. As observed in other downwelling regions the spectral energy of fluctuations decreased for the downwelling case compared to upwelling episodes (Federuik and Allen, 1996). Frequency search analysis carried out for two downwelling events showed that main oscillations were located at 15.7 hr (1.5-2.2 cm/s) and 16.9 hr in the CBL and 17.3 hr outside the CBL. Temperature data showed oscillations at 14.2 hr and 17.3 hr periodicity in the CBL; however, it was noticed that the amplitudes of these near-inertial oscillations were much smaller than during upwelling events.

4.3 *Along-shore momentum and cross-shore fluxes*

This analysis as well as past studies in Lake Ontario indicate that low frequency alongshore currents are primarily driven by alongshore winds (Csanady and Scott, 1980). The wind and current records during the upwelling and downwelling episodes were a valuable source for understanding the dynamics of alongshore flow. Neglecting alongshore momentum advection, the vertically integrated momentum balance for the alongshore current component can be given as

$$f\bar{v} = -\left[g\frac{\partial\eta}{\partial x} + \frac{g}{h\rho_o}\int_{-h}^{0}\frac{\partial\alpha}{\partial x}dz\right] + \frac{\tau_s}{\rho_o h} - \frac{\tau_b}{\rho_o h} \qquad (1)$$

where $\bar{v}$ is vertically integrated cross-shore velocity, f is the Coriolis force at 43.5° N, η is the deviation from static level, h is the local depth, g is gravitational acceleration and

$\alpha = \int_{-z}^{0} \rho dz$. The surface wind stress (τ_s) was given previously, and bottom stress is obtained by $\tau_b = C\rho_o|\bar{u}|\bar{u}$, C is a friction coefficient of $1.3X10^{-3}$ based on earlier studies. The vertically integrated currents were obtained from surface Lagrangian measurements and sub-surface currents meters and a few ship based measurements. Errors in depth-averaged velocity estimates include current and direction measurement errors. During both upwelling and downwelling events considerable shear was observed from 3.5 m to 10 m depths. Further, Lagrangian currents are accurate within 2-3 cm/s (Pal et al. manuscript submitted to *J. Geophys. Res.*, 1999). SACM current meters are extensively used in Lake Ontario studies, and their speeds are accurate to 0.5 cm/s with a lower threshold value of 0.2 cm/s. The ship based observations were not carried out at every hour. Two sets of measurements along the coastal chain were obtained for two to three days during each of these events. The density (ρ) at 30m depth (4 km from shore) was obtained (Chen and Millero, 1988) from the vertical profiles of temperature data which is accurate to the order of 0.1°C. Hence by assuming the uncertainty in the depth-averaged currents is on average 2 cm/s, the error in the Coriolis term will be $0.2x10^{-5}$ and uncertainty in calculating density could be as high as 0.1 kg/m^3. The alongshore slope was not measured in this study, but was obtained from the balance of other terms in the momentum equation.

The average values of alongshore momentum balance during upwelling show that the cross-shore current term ($0.7*10^{-5}$) was balanced by a combined barotropic and baroclinic pressure gradient ($0.51*10^{-5}$) and the wind stress ($0.15*10^{-5}$). The bottom stress was significantly small. The along-shore slope obtained in this study is consistent with earlier studies during summer stratification (Csanady and Scott, 1980; Simons and Schertzer, 1989) where the observed mean along-shore thermocline gradient was of the order of 5×10^{-5} which gave a surface level gradient of roughly 10^{-7} in the eastward direction. This suggests that during upwelling the Coriolis force associated offshore flow and the pressure gradient term are roughly in balance indicating that the flow seeks geostrophic equilibrium. However, during the downwelling episodes the along-shore momentum balance is more complicated. During this episode the cross-shore geostrophic current ($0.96*10^{-5}$) was in balance with combined contributions from pressure gradient ($0.4*10^{-5}$), wind stress ($0.36*10^{-5}$) and bottom stress ($0.19*10^{-5}$). The bottom stress was higher due to the increased mean currents in the downwelling.

Mean values of the products <u'v'> and <v'T'> represent the cross-shore transport of momentum and heat, respectively. During both upwelling and downwelling events the mean values of horizontal momentum and heat fluxes at 10 m depth were not statistically significant and were noisy. Near-inertial oscillations were probably responsible for this large scatter. By removing near-inertial oscillations between 18 hr and 14 hr using a band pass filter, we have observed weak off-shore transport in the FBL during upwelling episodes. Heat flux is negative in the IBL at this depth. During downwelling events significant negative fluxes were observed between 4 to 6 km in the coastal zone.

5.0 **Turbulent Exchange Coefficients**

Lagrangian Statistics

The methods of computing Lagrangian time scale, and eddy diffusion coefficients have been discussed by many authors (Poulain and Niiler, 1989; Dever et al., 1998). The Lagrangian integral time scale (T_i^L) and length scale (L_i^L) are the time and distance over which the drifter motion remains correlated are given by $T_i^L = \int_0^T R_{ii}^L(\tau)d\tau$ and

$L_i^L = \sqrt{\langle u_i'^2 \rangle} \int_0^T R_{ii}^L(\tau)d\tau$. Here, R_{ii}^L is the auto correlation function defined as

$$R_{ii}^L(\tau) = \frac{1}{T} \frac{\int_0^{T-\tau} u_i'(t)u_i'(t+\tau)dt}{< u_i'^2 >} \qquad (2)$$

where u′ is the residual velocity defined by u′=u-<u>, <.> denotes average over time. Further, it was observed that because of low frequency motions, Lagrangian integral time and length scales are generally time dependent and do not approach a constant limit. Most of the individual autocorrelation functions oscillate and have significant lobes which underestimate the integral time-scale as they are integrated over the duration of the time series. To avoid this, we follow the usual practice of integrating from zero to the time of first zero crossing.

Taylor (1921) showed that, in a stationary and homogeneous field of turbulence single particle dispersion is related to Lagrangian integral scale. Following earlier discussion it is assumed that the drifter velocity fluctuations are homogeneous and stationary as a first order approximation, and hence we can write the mean squared dispersion due to a particle motion as $\langle x_i'^2(t) \rangle = 2\langle u_i'^2 \rangle \int_0^t (t-\tau)R_{ii}^L(\tau)d\tau$. When diffusion time has elapsed beyond some lag time t_ℓ (Lagrangian correlation time scale), $R^L_{ii}(\tau)$ will drop to zero. Physically t_ℓ is the decay time scale of those eddies which contribute to diffusion. Therefore, for large time scales $t > t_\ell$ the horizontal eddy exchange coefficient is given by

$$K_i^L = \langle u_i'^2 \rangle T_i^L \qquad (3)$$

Eulerian statistics

In stationary and homogeneous turbulence, the Lagrangian variance $\langle u_L'^2 \rangle$ can be assumed to be equivalent to Eulerian variance $\langle u_e'^2 \rangle$ (Lumley and Panofsky, 1964). Hay and Pasquill (1959) also pointed out that the essential difference between Eulerian and Lagrangian velocities is that, at a fixed point, velocity fluctuations appear to move rather quickly, as turbulent eddies are advected past the instrument. They have shown that the Lagrangian correlation function $R_{ii}^L(\tau)$ and the Eulerian counterpart $R_e(\tau)$ have similar shape but differ only by a factor β which is greater than unity. $R_e(\tau) = R_{ii}^L(\beta\tau)$. Introducing these assumptions, the horizontal exchange coefficient in terms of Eulerian statistics can be written as

$$K_e = \beta \langle u_e'^2 \rangle T_e \qquad (4)$$

where T_e is the Eulerian integral time scale.

The autocorrelations for Lagrangian and Eulerian currents show a number of interesting features. An example of autocorrelations for a drifter (5385) and current meter (station 3) during an upwelling cycle were presented in figures 10 a&b. Similar patterns were observed for other locations. Autocorrelations of filtered Lagrangian velocities have fallen to near zero values for all drifters within 8-12 hours, and have shown peaks at 14 hr periodicity. The filtered Eulerian values shows a steady drop of alongshore autocorrelations, whereas cross-shore autocorrelations shows a peak at a period of 24 hr. Lagrangian time scales (τ_L) estimated from autocorrelations were less than Eulerian time (τ_e) scales. Similar characteristics were observed on the northern California shelf and in Santa Barbara channel

(Davis, 1985; Dever et al., 1998). This was attributed to the affect of total acceleration in Lagrangian measurements which includes advection, whereas Eulerian time scales were only function of local acceleration. This indicates the non-linearity of the evolution of time-varying currents.

Following Schott and Quadfasel, (1979) we have chosen $\beta = 1.4$ in eq (4) which may sometimes underestimate the horizontal exchange coefficients. However, this is a reasonable estimate as our primary goal is not the precise quantification of the exchange coefficient but the general analysis of various turbulence exchange characteristics. Since during the summer regime only Eulerian measurements were available, these values serve as an indicator of dispersal tendencies in the flow as well as to compare the influence of upwelling and downwelling episodes. The horizontal exchange coefficient values increased from 0.5 m^2/s to 48 m^2/s in the offshore direction.

Table 3 presents the horizontal exchange coefficients obtained by Eulerian and Lagrangian measurements during upwelling and downwelling episodes. The statistics show that alongshore exchange coefficients (K_x) were slightly higher than cross-shore components (K_y) in the first 5.5 km from the shore, i.e in the FBL. The cross-shore components reached a peak at around 6-7 km from shore and remained steady outside the CBL. These results indicate that momentum transfers occur in the longshore direction in the FBL and cross-shore transfers may dominate in the IBL. Although the magnitude of alongshore Lagrangian eddy coefficients were higher than Eulerian values, they show a peak nearly at the same distance. The cross-shore exchange coefficients in the surface levels were lesser than sub-surface values in the IBL. During downwelling the alongshore components were higher in the CBL, and outside the CBL the cross-shore exchanges were dominant. The turbulent momentum exchanges were rather small in the FBL, but significantly increased in the IBL. The exchange coefficients at 3.5 m depth from drifters have also shown higher alongshore values within the CBL. Both alongshore and cross-shore values increased rapidly to high values outside the CBL with increasing Lagrangian time scales. As observed in the upwelling case, the cross-shore exchange from Lagrangian measurements was smaller compared to Eulerian coefficients.

The turbulent exchange coefficients shows that during upwelling episodes, although alongshore coefficients were comparable to summer values, the cross-shore components increased, particularly in the IBL regime. It has been observed that lateral current shears are important in the FBL. This could be an important factor in the dispersion of material entered into lake waters. Since the mean currents and lateral shears decreased considerably during upwelling episodes, it is likely that short period fluctuations play an important role in the near-shore and cross-shore exchange processes. During downwelling episodes mean alongshore currents often exceeded 20 cm/s, which could result in alongshore water displacements of more than 100 km during the episode. Although turbulent exchange coefficients were small in the FBL, increased lateral shear may play a role in dispersing the material within the FBL.

6.0 Summary and Conclusions

This study presents an analysis of simultaneously observed time series data from six Eulerian current meters and from satellite tracked drifters for two experiments during the summer season in the coastal regions of Lake Ontario. Flow and structure of the coastal boundary layer along the north shore of Lake Ontario presents a complex scenario during upwelling and downwelling episodes under summer stratified conditions. The theoretical framework which has been created to explain these events comprises two kinds of models. The first model deals with the initial response of the lake to uniform wind stress, and the second type of model deals with the closed nature of the basins wherein transient response is described in terms of internal wave propagation (Simons and Schertzer, 1989). From the observations we have delineated elements of both theoretical models. The flow is divided into a mean (large scale) circulation and turbulent (near-inertial and other small scale fluctuations) oscillations on the basis of spectral minimum observed at 24 to 30 hours. Following earlier studies (Csanady, 1972; Murthy and Dunbar, 1980) in the Great Lakes we have delineated the CBL into a FBL with a width of ~3 km and an IBL of 5-6 km width during summer stratification. These flow regimes varied significantly in upwelling and downwelling episodes.

The observed circulation within the FBL was predominantly shore parallel, while further offshore the flow was dominated by near-inertial oscillations. The summer regime was characterized by an increase in turbulence intensity with increased distance from shore. Alongshore winds were mainly responsible for low frequency motion in the CBL, however, some instances were identified where cross-shore component of the winds influenced the near-inertial oscillations of the coastal circulation. The net flow (3-4 cm/s) and thermal gradients between coastal stations and offshore stations confirm the earlier studies that the flow seeks geostrophic equilibrium (Csanady, 1982).

During this experimental period temperature variations were dominated by the influence of a few short wind events. The eastward (westward) wind stress caused thermocline elevation (depression). The upwelling events were characterized by relatively weaker eastward flow (~5 cm/s), and downwelling events with strong westward currents (20-

30 cm/s), with each episode lasting for about 4 to 6 days. The results show inferences to the propagation of internal Kelvin waves due to the thermocline oscillations within the CBL.

South-eastward transport in surface levels of the FBL and weak onshore flow just below the surface mixed layer in the IBL were observed during upwelling episodes. Alongshore vertically integrated momentum balance shows quasi-geostrophic equilibrium. These results are consistent with earlier observations in Lake Ontario (Csanady and Scott, 1980) and other coastal upwelling regions (Davis, 1985; Lentz, 1992; Allen et al., 1995). No coastal jet was observed during this upwelling episode. The sub-surface currents showed considerable increase in turbulence intensity due to increased near-inertial and decreased mean scalar current speeds. During the upwelling the peak turbulence intensity as well as total kinetic energy were slightly shifted inshore. The width of the FBL increased to 5.5 km and the IBL width decreased to 3.5 km. Upwelling events were also characterized by dominance of turbulent kinetic energy in the CBL. During these episodes momentum transfer occurred in the alongshore direction in the FBL, but cross-shore momentum transfer dominated in the IBL. In contrast to the earlier observations (Blanton, 1975) this study shows that a wave of 16-hr periodicity is more dominant than 17-hr and 14-hr waves during upwelling.

During downwelling episodes a coastal jet was observed in deeper levels with peak speeds of 20-30 cm/s at 3 km from the shore. This is consistent with earlier observations in Lake Ontario (Simons and Schertzer, 1989) as well as on the Oregon continental shelf (Allen and Newberger, 1996). The turbulent intensities decreased significantly in comparison to the summer regime. During the downwelling the width of the CBL increased to 14-15 km with the IBL extending over 10 km. The along-shore exchange coefficients were slightly higher in the FBL, but cross-shore exchanges became important in the IBL. Downwelling episodes were also characterized by less contribution from the TKE. Relatively weaker short period oscillations at 15.7-hr and 16.9-hr due to baroclinic seiches in the FBL, and 17.3 hr due to inertial motion, were observed in the outer boundary layer.

Acknowledgements

The authors wish thank Dr. Badal Pal for calculating some parts of Lagrangian statistics, Ken Miners for his support in organizing and presenting the data. Comments and suggestions from anonymous reviewers greatly improved the manuscript. One of the authors (Y.R) is supported by Natural Sciences and Engineering Council (NSERC) Visiting Fellow Programme.

References

Adeney, K.M., and M.J. Korenberg., 1994: Fast orthogonal search for array processing and spectrum estimation., *IEEE -Vis. image and sig. process.*, 141, 13-18.

Allen, J.S., and P.A. Newberger, 1996: Downwelling circulation on the Oregon continental shelf, Part 1: Response of idealized forcing, *J. Phys. Oceanogr.*, 26, 2011-2035.

_____, _____, and J. Federuik, 1995: Upwelling circulation on the Oregon continental shelf, Part 1: Response to idealized forcing, *J. Phys. Oceanogr.*, 25, 1843-1866.

Beletsky, D, W.P. O'Connor, D.J. Schwab & D.E. Dietrich, 1997 :Numerical simulation of internal Kelvin waves and coastal upwelling fronts; *J. Phys. Oceanogr.*, 27, 1197-1215.

Blanton, J.O., 1975: Nearshore lake currents measured during upwelling and downwelling of the thermocline in Lake Ontario; *J. Phys. Oceanogr.*, 5, 111-124.

Bogucki, D., T. Dickey and L.G. Redekopp, 1997: Sediment resuspension and mixing by resonantly generated internal solitary waves, *J. Phys. Oceanogr.*, 27, 1181-1196.

Boyce, F.M., M.A. Donelan, P.F. Hamblin, C.R. Murthy, and T.J. Simons, 1989: Thermal structure and circulation in Great Lakes., *Atmos-Ocean*, 27(4), 607-642.

Brink, K.H., D. Halpern, and R.L. Smith., 1980: Circulation in the Peruvian upwelling system near 15°S., *J. Geophys. Res.*, 85, 4036-4048.

Chen, C.T. and F.J. Millero, 1986: Precise thermodynamic properties of natural waters covering only Limnological range, *Limnol. Oceanogr.*, 31, 657-662.

Csanady, G.T., 1972: The coastal boundary layer in Lake Ontario, 2, The summer-fall regime, *J. Phys. Oceanogr.*, 2, 168-176.

____, 1982: Circulation in the Coastal Ocean, D. Reidel Publishing Company, Dordrecht, Holland, pgs: 279.

_____, and J.T. Scott, 1980: Mean summer circulation in Lake Ontario within the coastal zone, *J. Geophys. Res.*, 85, 2797-2812.

Davidson, F.M., R.J. Greatbach, and A.D. Goulding; 1998: On the net cyclonic circulation in large stratified lakes., *J. Phys. Oceanogr.*, 28, 527-534.

Davis, R.E., 1985: Drifter observations of coastal surface currents during CODE: The method and descriptive view, *J. Geophys. Res.*, 90, 4741-4755.

_____, 1991: Observing the general circulation with floats, *Deep Sea Res.*, part I, 38, S531-S571.

Dever, E.P. M.C. Hendershott, and C.D. Winant; 1998: Statistical aspects of surface drifter observations of circulation in the Santa Barbara channel, *J. Geophys. Res.*, 103, 24781-24797.

Emery, K.O., and G.T. Csanady, 1973: Surface circulation of lake and nearly land locked seas, *Proc. Natl. Acad. Sci., USA*, 70, 93-97.

Federiuk, J., and J.S. Allen, 1996: Model studies of near-inertial waves in flow over the Oregon continental shelf., *J. Phys. Oceanogr.*, 26, 2053-2075.

Graham, R.J., 1963: Determination and analysis of numerical smoothing weights, NASA Tech and Res. No 179, 28 pp.

Hay, J.S and F. Pasquill, 1959: Diffusion from a continuous source in relation to spectrum and scale of turbulence, *Adv. in Geophys.*, 6, 345-365.

Ivey, G.N., 1987: The role of boundary mixing in the deep ocean., J. *Geophys. Res.*, 90, 7256-7264.

Lee, C.H. and N. Hawley, 1998: The response of suspended particulate material to upwelling and downwelling events in southern lake Michigan, *J. Sedimentary Res.*, 68, 819-831.

Lentz, S.J., 1992: The surface boundary layer in coastal upwelling regions, *J. Phys. Oceanogr.*, 22, 1517-1539.

_____, 1995: Sensitivity of the inner-shelf circulation to the form of eddy viscosity profile, *J. Phys. Oceanogr.*, 25, 19-28.

Lumley, L. and H.A. Panofsky, 1964: The structure of atmospheric turbulence, Interscience, NewYork.

Mortimer, C.H., 1977: Internal waves observed in Lake Ontario during IFYGL 1972: Description survey and preliminary interpretation of near inertial oscillations, Centre for Great lake studies, Univ of Wisconsin-Milwaukee, Pgs. 122.

Murthy C.R. and D.S. Dunbar, 1981: Structure of flow within the coastal boundary layer of the Great lakes, *J. Phys. Oceanogr.*, 11, 1567-1577.

Niiler, P.P., A.S. Sysbrandy, K. Bi, P.M. Poulain, and D. Bitterman, 1995: Measurements of the water following capability of Holey-Sock and Tristar drifters, *Deep Sea Res.*, 42, 1951-1964.

Poulain, P.M., and P.P. Niiler, 1989: Statistical analysis of the surface circulation of the California current system using satellite-tracked drifters, *J. Phys. Oceanogr.*, 19, 1588-1603.

Schott, F and D. Quadfasel, 1979: Lagrangian and Eulerian measurements of horizontal mixing in the Baltic, *Tellus*, 31, 138-144.

Schwab, D.J., 1977: Internal free oscillations in Lake Ontario, *Limnol. Oceanogr.*, 22, 700-708.

_____, W.P. O'Connor and G. Mellor, 1995: On the net cyclonic circulation in large stratified lakes. *J. Phys. Oceanogr.*, 25, 1516-1520.

Simons, T.J., 1974: Verification of numerical models of Lake Ontario. Part 1: Circulation in spring and early summer. *J. Phys. Oceanogr.*, 4, 507-523.

_____, and W.M. Schertzer, 1989: The circulation of Lake Ontario during summer of 1982 and the winter of 1982/83, Scientific series, 171, National Water Research Institute, CCIW, Burlington, Pgs. 191.

Smith, R.L., 1981: A comparison of structure and variability of the flow field in three coastal upwelling regions: Oregon, northwest Africa and Peru., Coastal upwelling, F.A. Richards, Ed., *Amer. Geophys. Union*, 107-118.

Taylor G.I., 1921: Diffusion by continuous movements, *Proc. London Math Soc.*, 20, 196-212.

Winant, C.D., R.C. Beardsley, and R.E. Davis, 1987: Moored wind, temperature and current observations made during CODE-1 and CODE-2 over northern California shelf and upper slope, *J. Geophys. Res.*, 92, 1569-1604.

Wunsch, C., 1970: On the oceanic boundary mixing, *Deep-Sea Res.*, 17, 293-301

List of Figures

List of Tables

Eulerian					Lagrangian				
Station	U_E (cm/s)	V_E (cm/s)	$u_{rms(E)}$ (cm/s)	$v_{rms(E)}$ (cm/s)	Drifter	U_L (cm/s)	V_L (cm/s)	$u_{rms(L)}$ (cm/s)	$v_{rms(L)}$ (cm/s)
1	-0.36	-0.23	0.86	1.29	1	5.71	-1.79	6.61	6.13
2	1.44	-0.35	3.27	2.67	2	8.90	-2.83	9.32	6.59
3	0.83	0.43	4.79	3.95	3	2.23	-2.47	7.84	8.64
4	.34	0.06	3.85	4.35	4	2.51	-2.66	6.35	5.71
5	0.02	0.21	4.17	4.33	5	3.83	-4.43	6.68	6.21
6	2.78	-0.58	4.79	4.43	6	6.86	-3.55	8.62	6.78

Table 1 : Mean and rms velocities of Eulerian and Lagrangian measurements during upwelling cycle

Eulerian					Lagrangian				
Station	U_E (cm/s)	V_E (cm/s)	$u_{rms(E)}$ (cm/s)	$v_{rms(E)}$ (cm/s)	Drifter	U_L (cm/s)	V_L (cm/s)	$u_{rms(L)}$ (cm/s)	$v_{rms(L)}$ (cm/s)
1	-3.75	-0.09	1.45	1.18	1	0.66	0.15	5.0	2.78
2	-11.89	0.07	3.32	2.61	2	1.0	0.03	9.32	5.68
3	-9.99	2.98	5.48	4.78	3	1.61	0.06	7.99	5.17
4	-8.98	-0.12	5.47	5.50	4	-2.48	1.38	13.0	8.7
5	-6.58	-2.02	6.16	6.50	5	-8.23	0.01	17.5	11.0
6	-4.35	-2.72	7.60	8.36	6	-6.92	1.36	18.1	12.8

Table 2 : Mean and rms velocities of Eulerian and Lagrangian measurements during downwelling cycle

Station/ Distance from shore (km)	$K_{x(E)}$ X 10^5 cm^2/s	$K_{y(E)}$ X 10^5 cm^2/s	Drifter bin	$K_{x(L)}$ X 10^5 cm^2/s	$K_{y(L)}$ X 10^5 cm^2/s
Upwelling					
1 /0.68	0.277	0.864	1	7.13	5.92
2 /3.24	10.36	6.173	2	68.8	10.2
3 /5.42	26.98	16.78	3	15.5	2.02
4 /7.30	16.62	20.38	4	3.47	2.28
5 /9.28	19.26	20.42	5	17.5	6.43
6 /14.2	24.30	20.33	6	27.8	2.75
Downwelling					
1 /0.68	1.010	0.652	1	6.51	0.35
2 /3.24	7.161	4.197	2	23.1	3.43
3 /5.42	30.97	21.55	3	14.7	4.10
4 /7.30	31.16	28.42	4	83.2	11.6
5 /9.28	37.03	41.57	5	223.2	31.9
6 /14.2	60.09	72.37	6	223.6	48.8

Table 3 : Alongshore (K_x) and cross-shore (K_y) eddy diffusivities from Eulerian and Lagrangian measurements during upwelling and downwelling cycles (subscript L indicates Lagrangian and E indicates Eulerian measurements).

Lake Ontario Current Meter
Port Darlington, NGS 1990

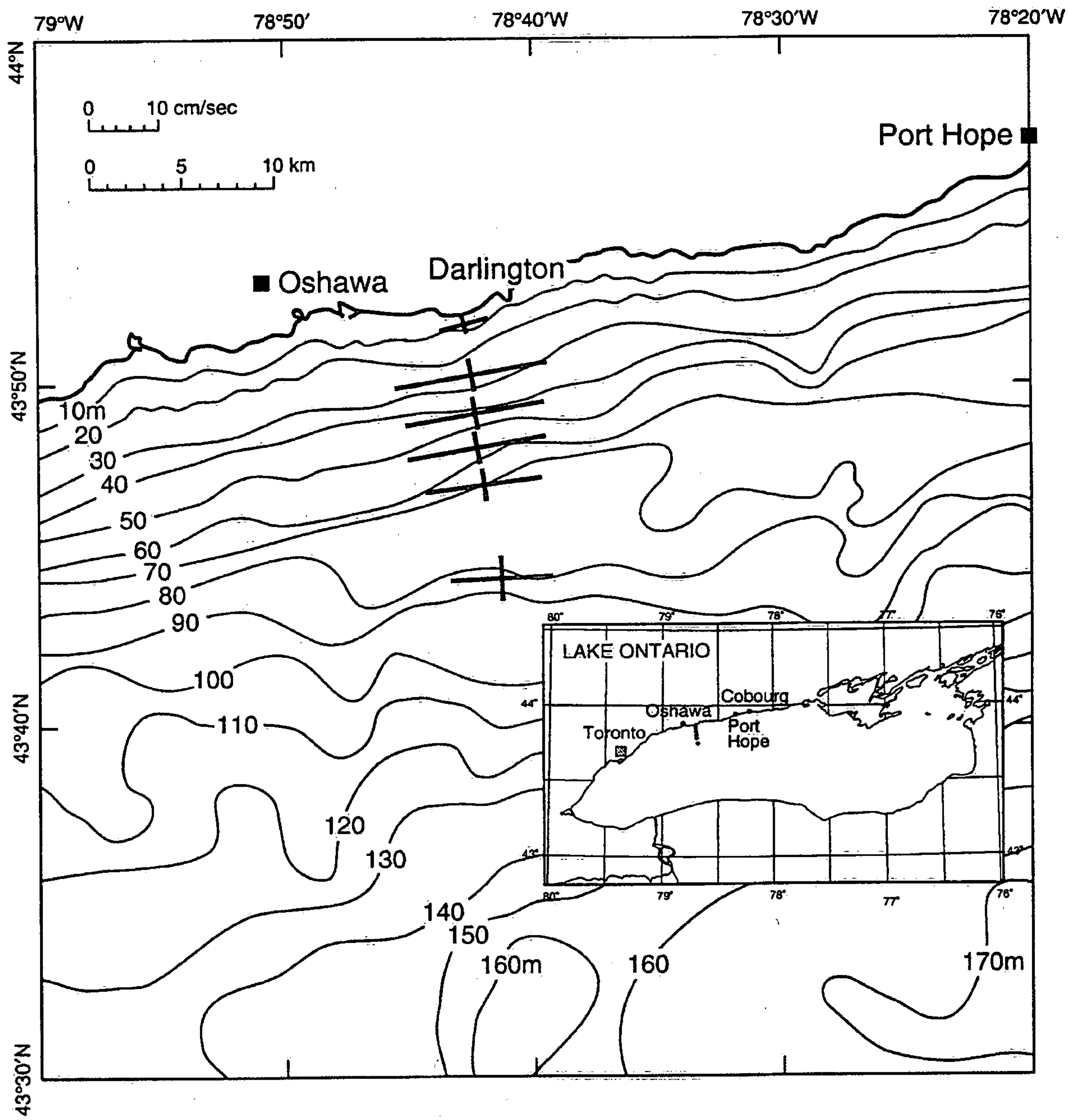

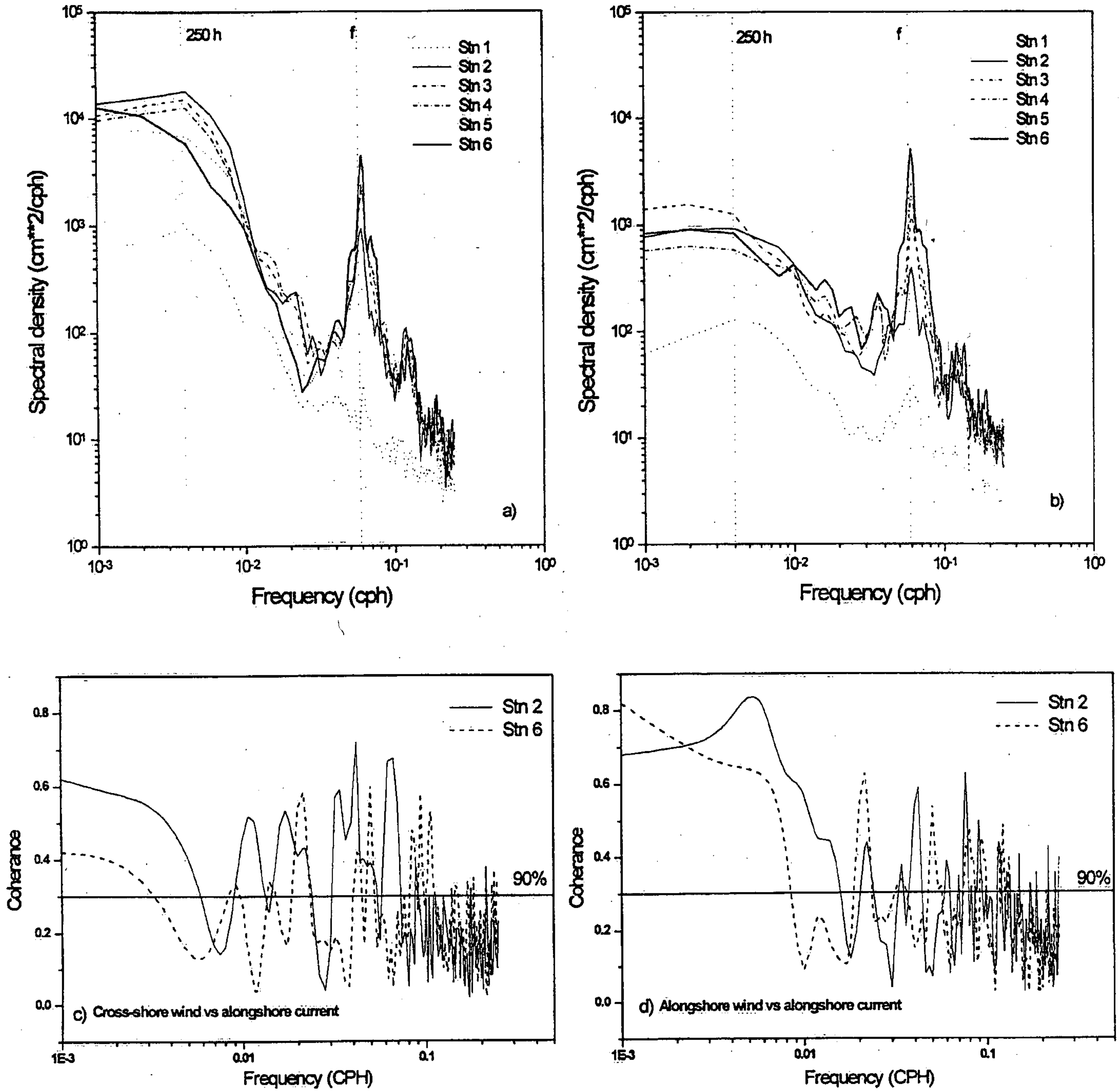
250 h
f
Stn 1
Stn 2
Stn 3
Stn 4
Stn 5
Stn 6
Spectral density (cm**2/cph)
Frequency (cph)
a)
b)
Coherance
Frequency (CPH)
90%
c) Cross-shore wind vs alongshore current
d) Alongshore wind vs alongshore current

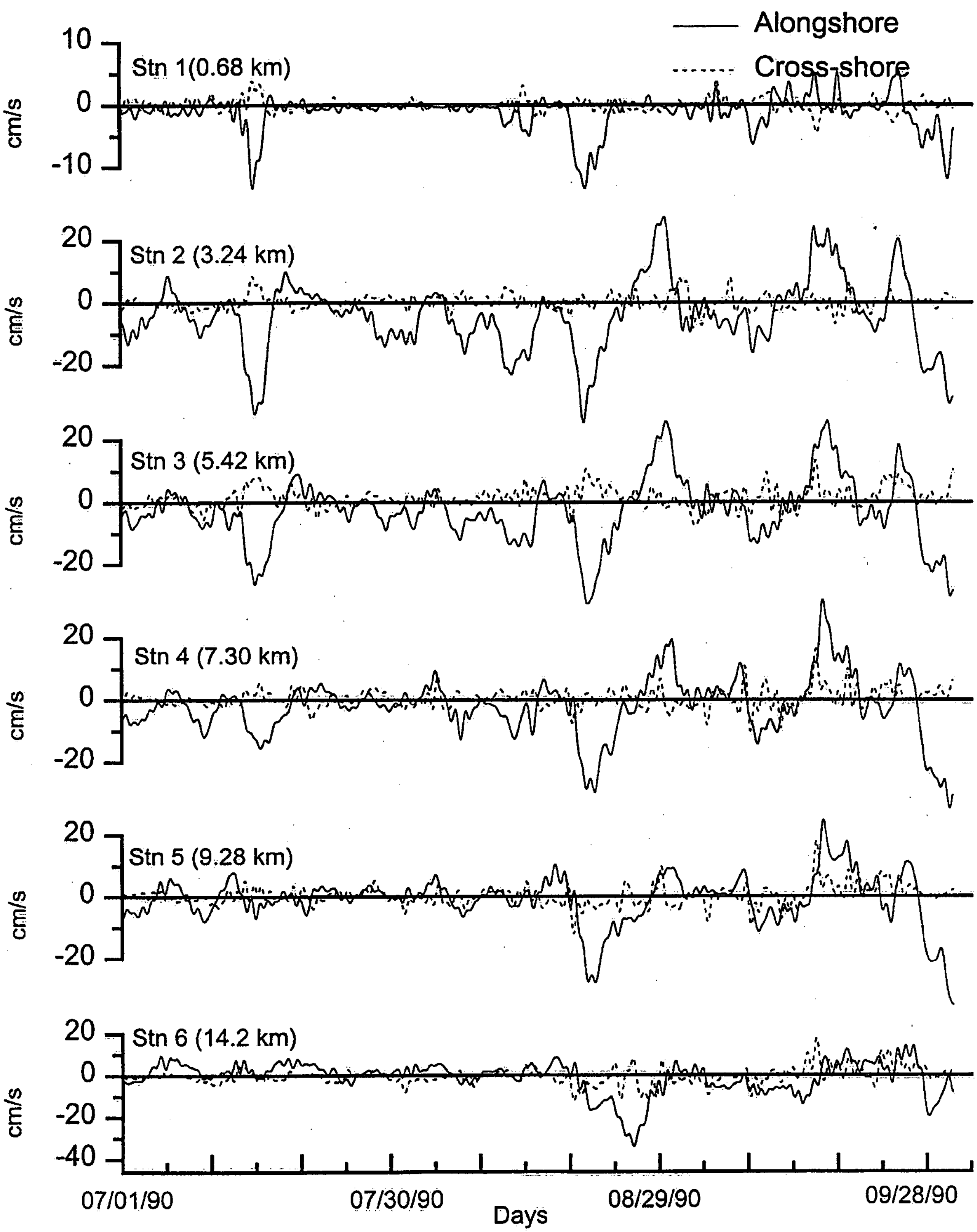
Alongshore
Cross-shore
Stn 1(0.68 km)
Stn 2 (3.24 km)
Stn 3 (5.42 km)
Stn 4 (7.30 km)
Stn 5 (9.28 km)
Stn 6 (14.2 km)
cm/s
10
0
-10
20
-20
-40
07/01/90
07/30/90
08/29/90
09/28/90
Days

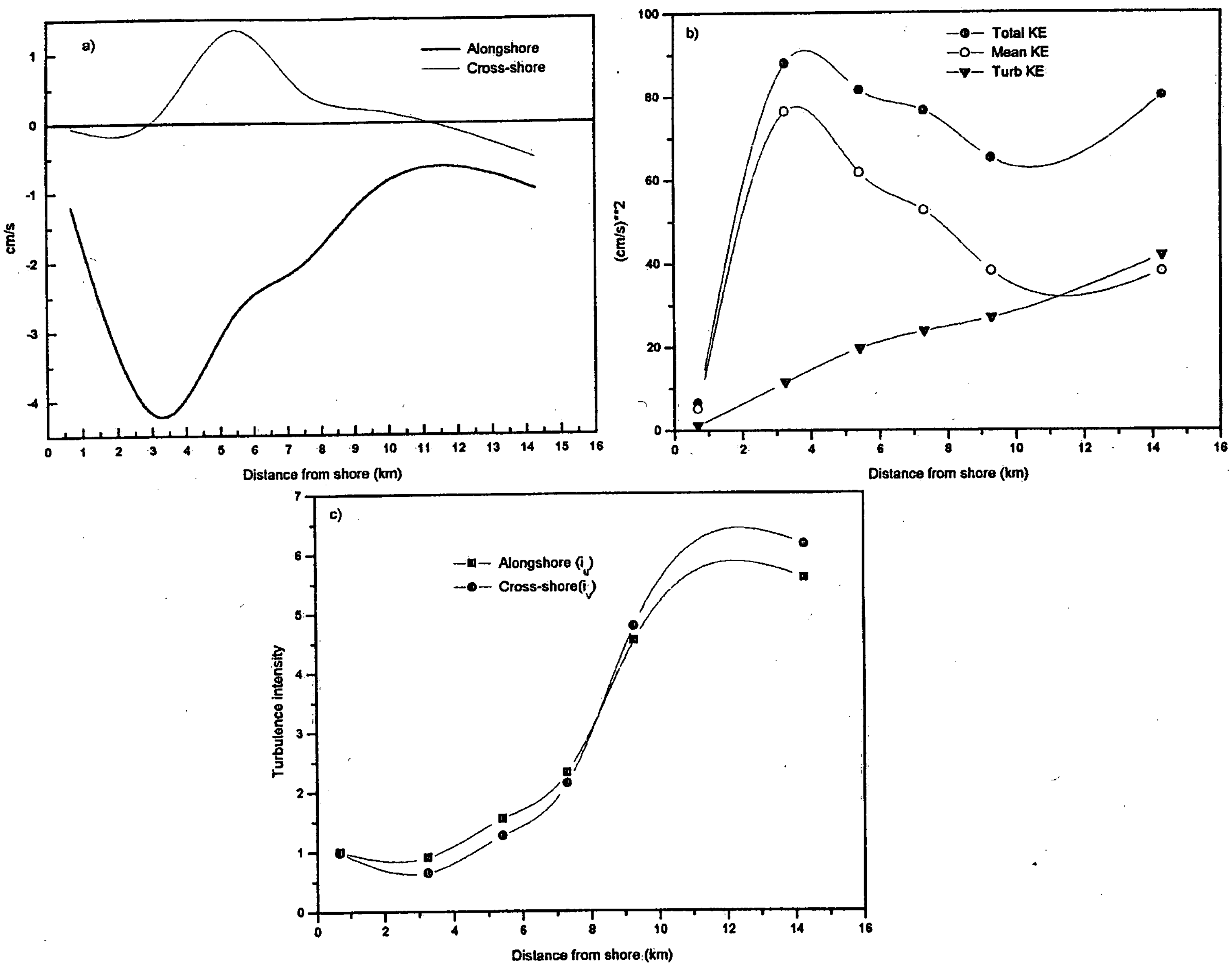
a)
Alongshore
Cross-shore
cm/s
Distance from shore (km)
b)
Total KE
Mean KE
Turb KE
(cm/s)**2
Distance from shore (km)
c)
Alongshore (i_u)
Cross-shore(i_v)
Turbulence intensity
Distance from shore (km)

4

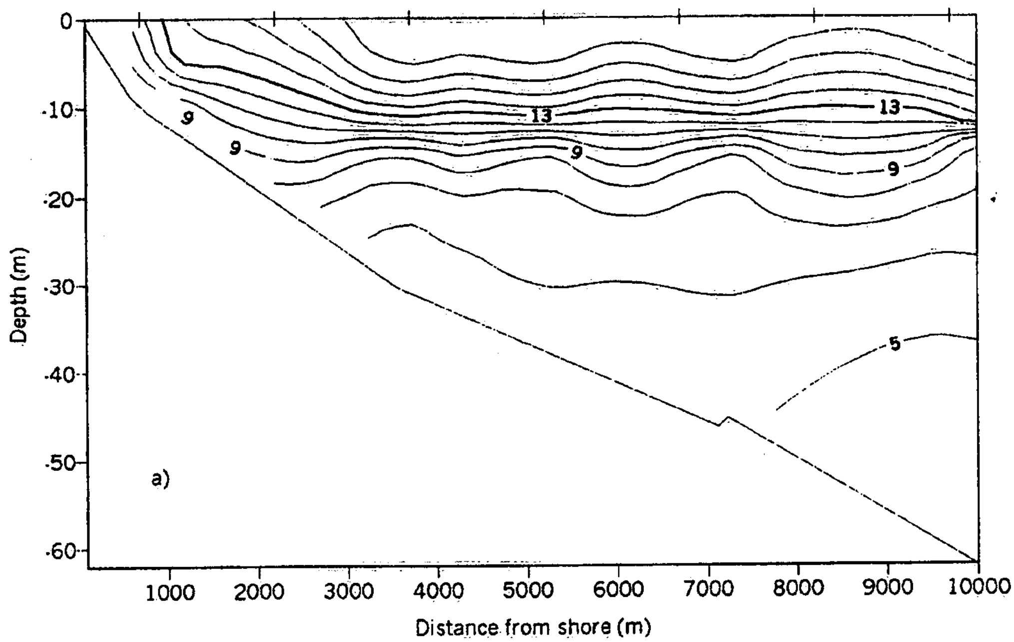
0
-10
-20
-30
-40
-50
-60
Depth (m)
9
9
13
13
9
9
5
a)
1000
2000
3000
4000
5000
6000
7000
8000
9000
10000
Distance from shore (m)

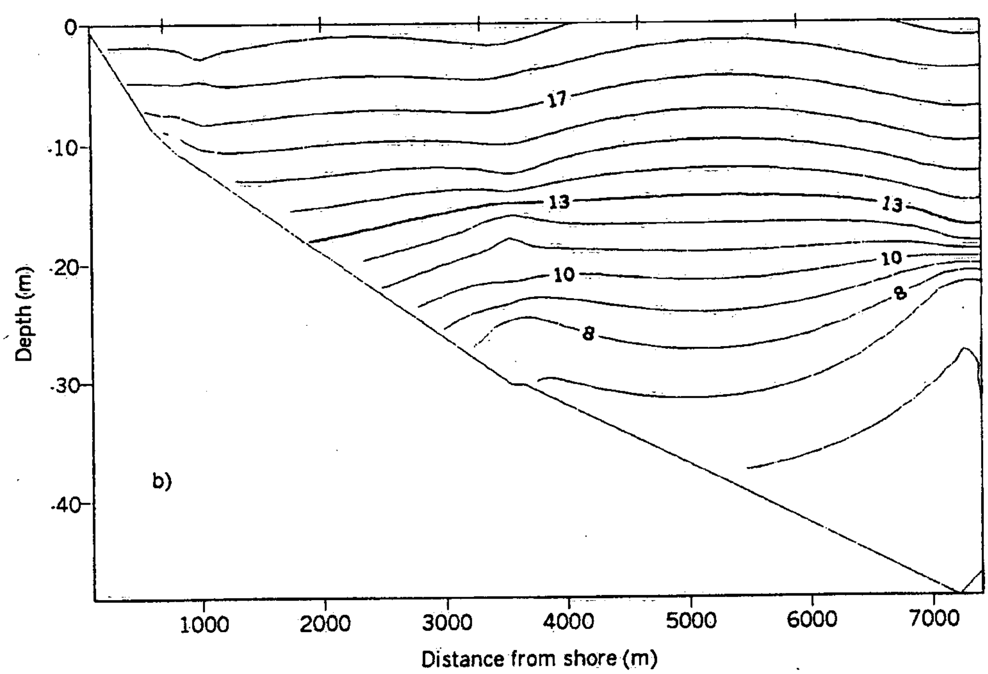
0
-10
-20
-30
-40
Depth (m)
17
13
13
10
10
8
8
b)
1000
2000
3000
4000
5000
6000
7000
Distance from shore (m)

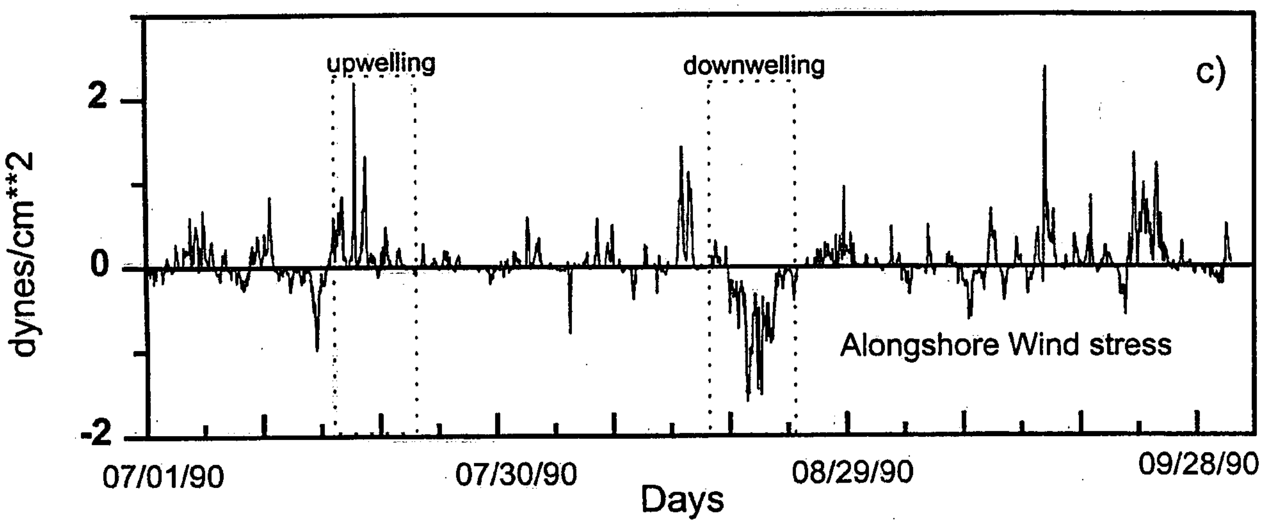
upwelling
downwelling
c)
2
0
-2
dynes/cm**2
Alongshore Wind stress
07/01/90
07/30/90
08/29/90
09/28/90
Days

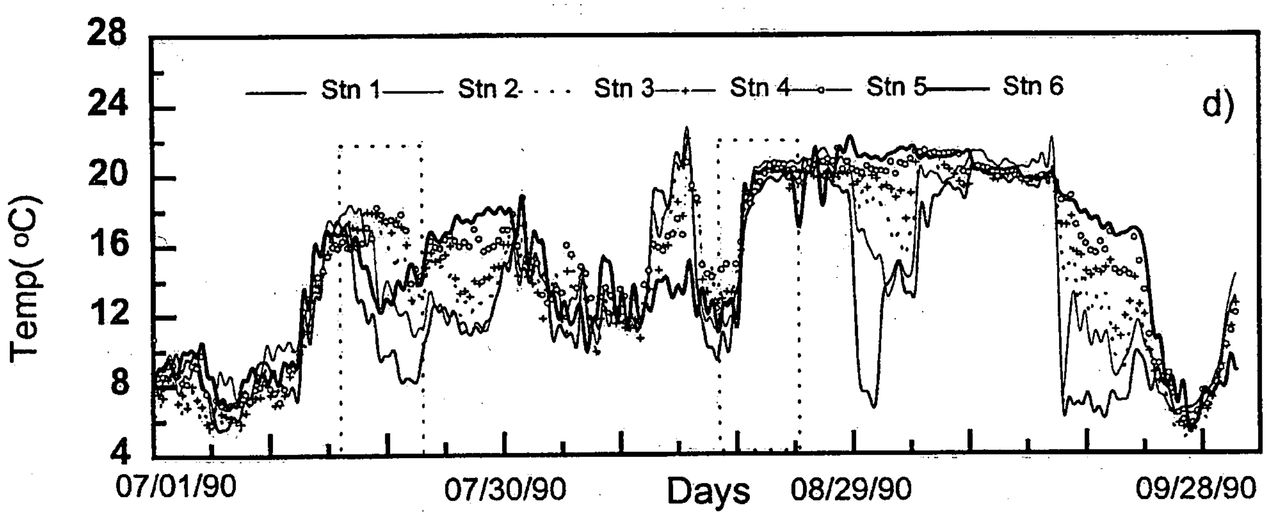
28
24
20
16
12
8
4
Stn 1
Stn 2
Stn 3
Stn 4
Stn 5
Stn 6
d)
Temp(oC)
07/01/90
07/30/90
Days
08/29/90
09/28/90

Lake Ontario Drifter

Darlington, Expt3, 1990.

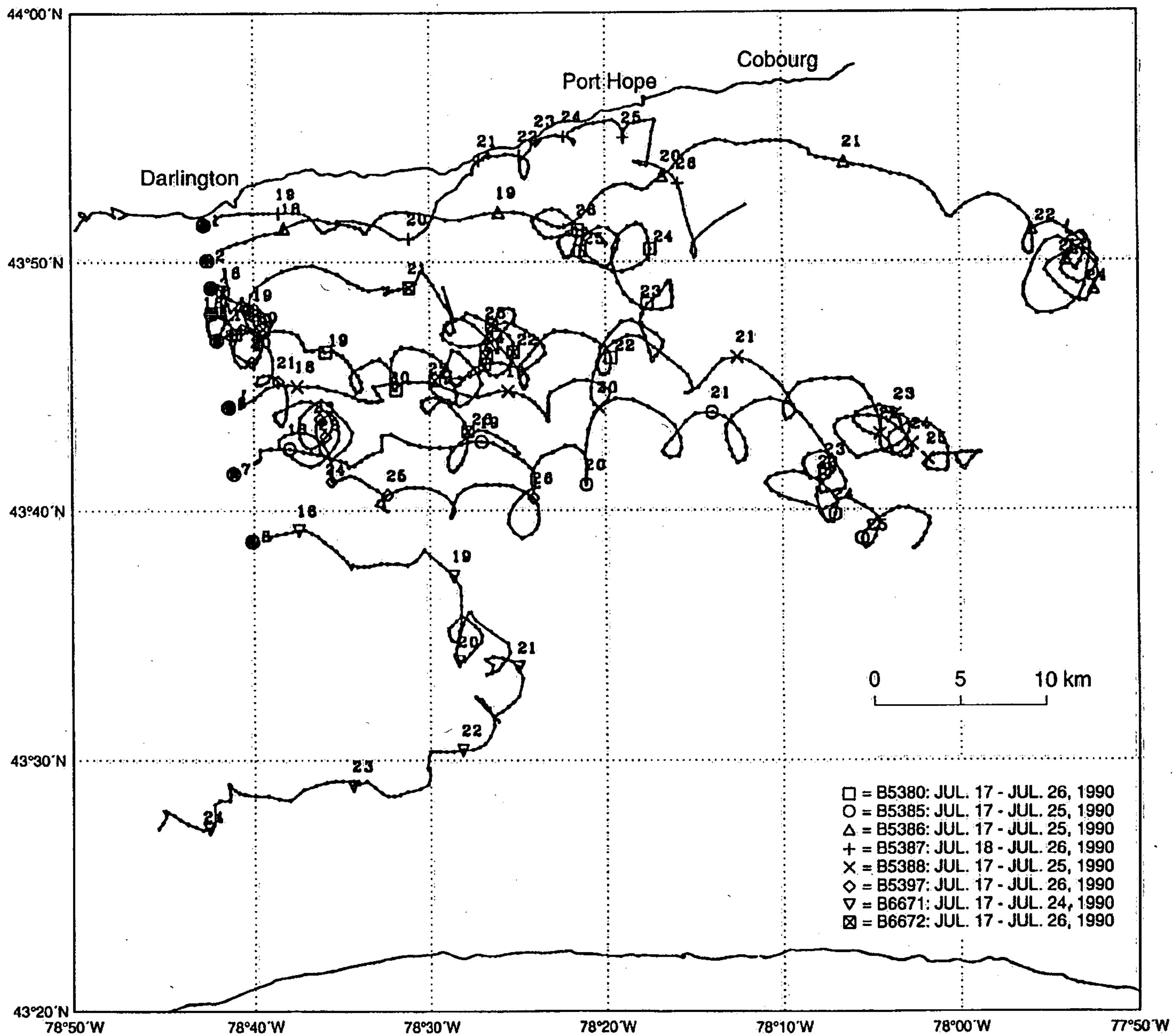

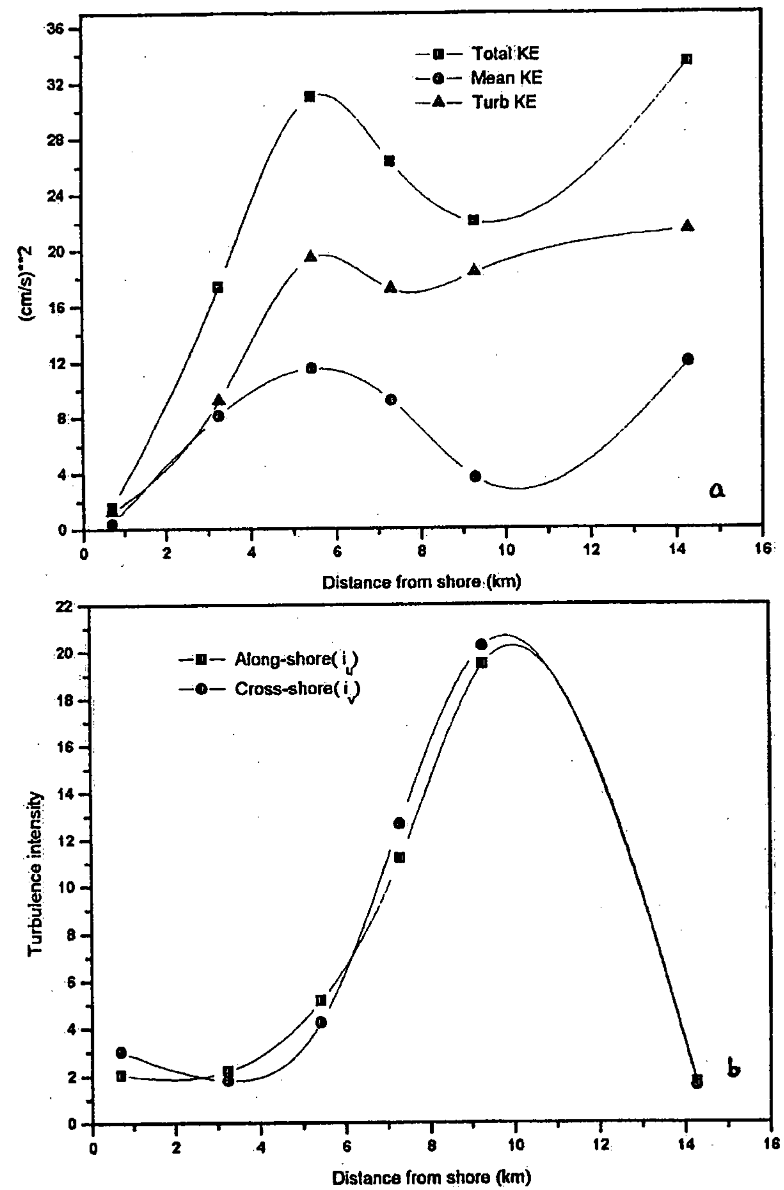

Total KE
Mean KE
Turb KE
(cm/s)**2
Distance from shore (km)
a
Along-shore(i_u)
Cross-shore(i_v)
Turbulence intensity
Distance from shore (km)
b

Lake Ontario Drifter

Darlington, Expt4, 1990.

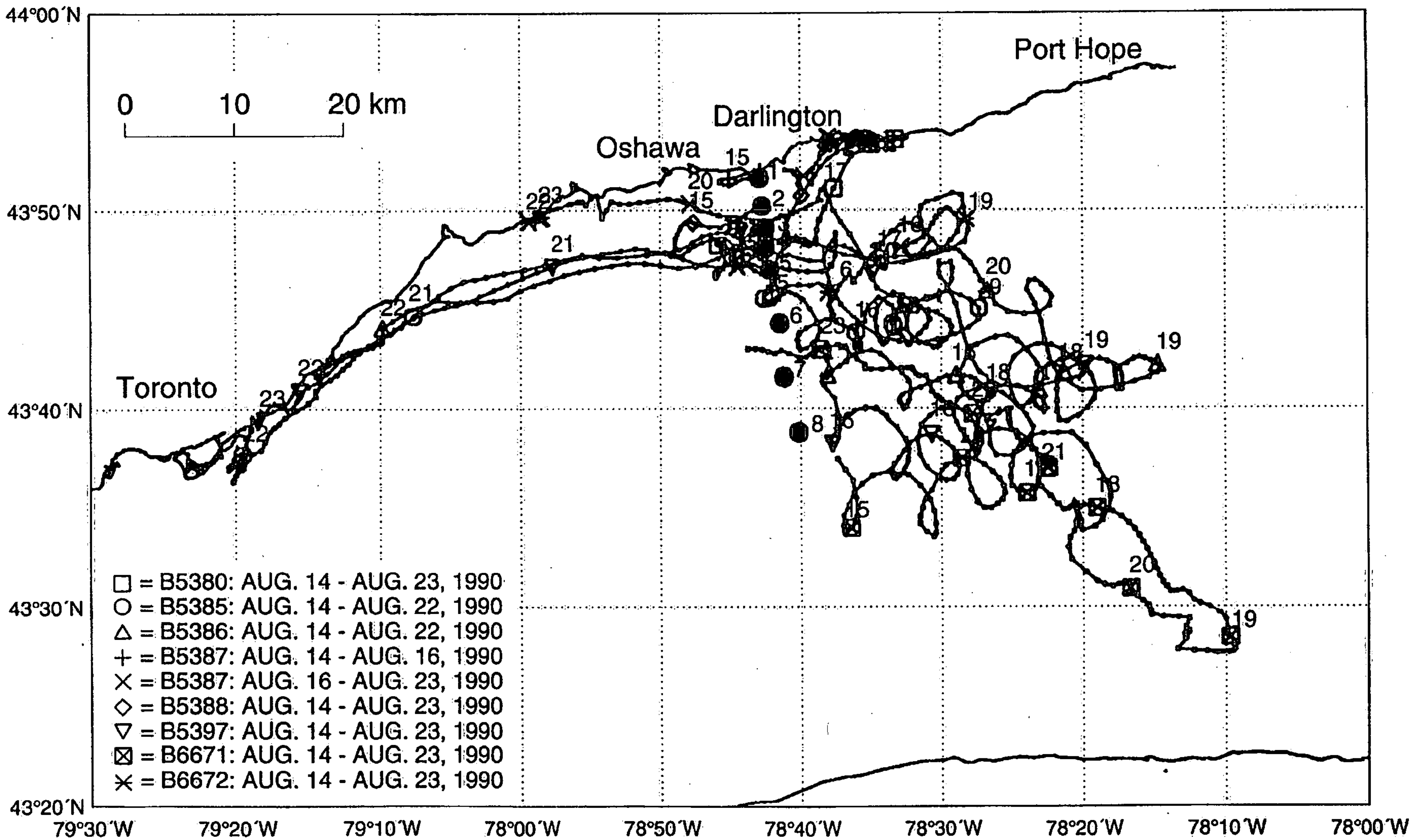

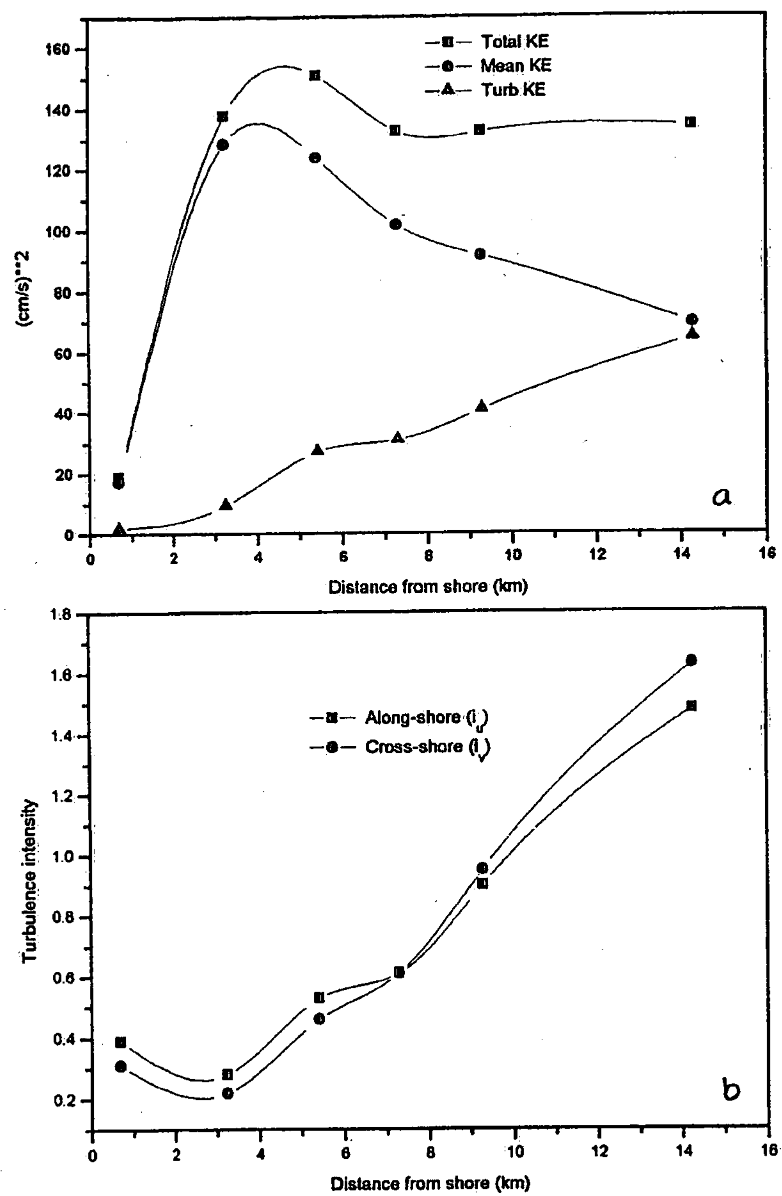
Total KE
Mean KE
Turb KE
(cm/s)**2
Distance from shore (km)
a
Along-shore (i_u)
Cross-shore (i_v)
Turbulence intensity
Distance from shore (km)
b

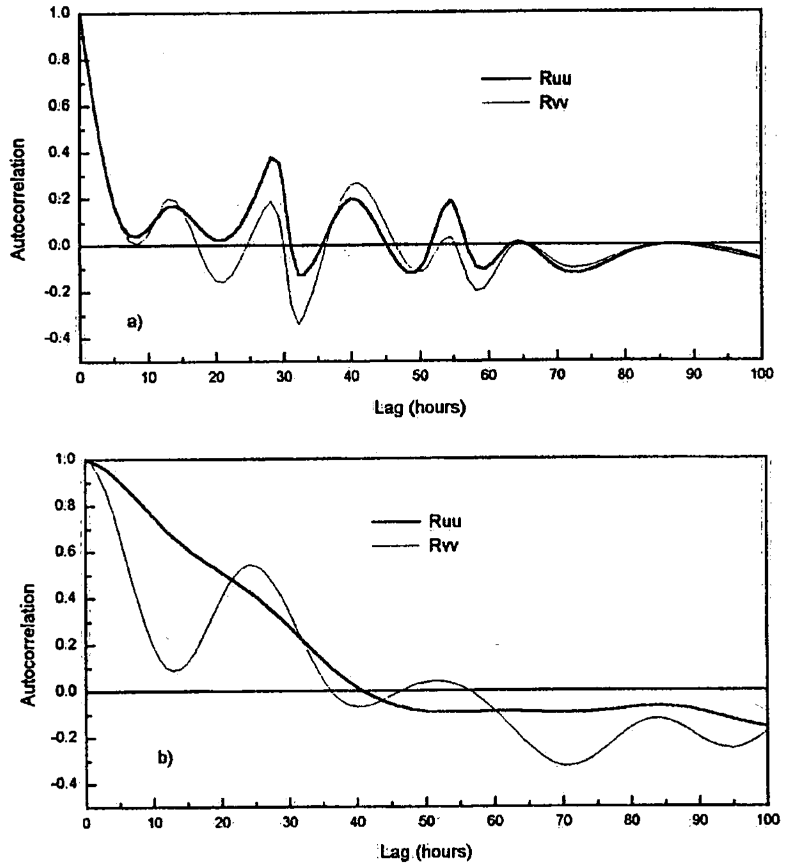
Ruu
Rvv
Autocorrelation
a)
Lag (hours)
Ruu
Rvv
Autocorrelation
b)
Lag (hours)

Environment Canada Library, Burlington
3 9055 1017 5537 8

Environment Canada Environnement Canada

Canada

Canada Centre for Inland Waters
P.O. Box 5050
867 Lakeshore Road
Burlington, Ontario
L7R 4A6 Canada

National Hydrology Research Centre
11 Innovation Boulevard
Saskatoon, Saskatchewan
S7N 3H5 Canada

St. Lawrence Centre
105 McGill Street
Montreal, Quebec
H2Y 2E7 Canada

Place Vincent Massey
351 St. Joseph Boulevard
Gatineau, Quebec
K1A 0H3 Canada

Centre canadien des eaux intérieures
Case postale 5050
867, chemin Lakeshore
Burlington (Ontario)
L7R 4A6 Canada

Centre national de recherche en hydrologie
11, boul. Innovation
Saskatoon (Saskatchewan)
S7N 3H5 Canada

Centre Saint-Laurent
105, rue McGill
Montréal (Québec)
H2Y 2E7 Canada

Place Vincent-Massey
351 boul. St-Joseph
Gatineau (Québec)
K1A 0H3 Canada